# Application of wastewater and environmental surveillance for pathogenic agents during the 2024 National Football League (NFL) Draft in Detroit, Michigan (USA)

Ryland Corchis-Scott[1], Ethan Harrop[1], Qiudi Geng[1], Mackenzie Beach[1], John Norton[2], Mehdi Aloosh[3,4], Thomas Reid[5], Rajesh Seth[6], Christopher G. Weisener[1], and R. Michael McKay[1]

Author affiliations:

[1]University of Windsor, Great Lakes Institute for Environmental Research, Windsor, Ontario, Canada

[2]Great Lakes Water Authority, Detroit, MI, United States

[3]Windsor-Essex County Health Unit, Windsor, Ontario, Canada

[4]Department of Health Research Methods, Evidence, and Impact, McMaster University, Hamilton, Ontario

[5]Environment and Climate Change Canada, Canada Centre for Inland Waters, Burlington, Ontario, Canada

[6]University of Windsor, Department of Civil and Environmental Engineering, Windsor, Ontario, Canada

Corresponding author: Ryland Corchis-Scott, Great Lakes Institute for Environmental Research, University of Windsor, 401 Sunset Ave., Windsor, ON, Canada N9B 3P4; corchisr@uwindsor.ca, 519-991-3493

## Abstract

Mass gatherings pose a concern for public health because they are associated with dense crowds, increased social interaction, and travel, all of which can facilitate the rapid transmission of infectious diseases. Wastewater and environmental surveillance (WES) were used for pathogen monitoring during the 2024 NFL Annual Player Selection Meeting (the 'Draft') in Detroit, MI, an event that drew an estimated 775,000 attendees. Wastewater and environmental samples were queried for respiratory viruses and clinically relevant ARGs. WES did not detect an increase in the concentration of monitored respiratory viruses (SARS-CoV-2, IAV, IBV, and RSV) associated with the 2024 NFL Draft. In contrast, WES detected a transient increase in carbapenemase targets in wastewater, primarily driven by a fourfold increase in $bla_{OXA-48}$. Resistome structure in wastewater was dominated by sampling site characteristics rather than changes associated with the event. The Draft weekend coincided with rainfall-driven combined sewer overflow (CSO), potentially allowing the dissemination of antimicrobial resistance genes (ARGs) to the environment. In surface waters receiving wastewater effluent, an increase in detection frequency and normalized concentrations for multiple ARGs were observed following the Draft. WES provided an overview of pathogen prevalence before, during, and after a large-scale gathering, showing how it can warn of emerging health risks in near real time.

## Introduction

Analysis of wastewater can provide information that accurately reflects infectious diseases dynamics[1–3] by integrating signals from symptomatic, subclinical, and asymptomatic individuals[4–7]. Wastewater and environmental surveillance (WES) is not a new discipline, but it has experienced a renaissance following its successful implementation during the COVID-19 pandemic[8–10]. Increased interest in WES has been driven by the numerous advantages it offers, including correlation with clinical metrics[11–17], cost-effectiveness[18–21], independence from test-seeking behaviour or availability of testing infrastructure[22], scalability from building to city levels[14,23–25], and timeliness with near real-time data generation[12,26,27].

An emerging application of WES is infectious diseases surveillance during mass gatherings[28]. Mass gatherings are typically large, planned events that concentrate individuals from diverse geographies into dense settings with high mobility, conditions that facilitate the transmission of infectious diseases[29]. Mass gatherings pose a challenge to epidemiological disease tracking due to travel and increased likelihood of rapid transmission. Disease surveillance before, during and after events allows for rapid response to widespread transmission following disease detection[28,30]. WES offers an effective means by which populations may be monitored surrounding large-scale gatherings such as sporting events[31–33].

Prior applications of WES to mass gatherings have targeted SARS-CoV-2 to monitor transmission of COVID-19 and include the 2020 Tokyo Olympics[34], the Two Oceans Marathon in South Africa[35], and the 2022 FIFA World Cup in Qatar[36]. Recent festival-based monitoring in New Orleans, LA, expanded the application of WES to mass gatherings, where it was implemented to target Mpox transmission[37]. Beyond respiratory viruses, surveillance of antimicrobial resistance (AMR) via antimicrobial resistance genes (ARGs) is gaining traction, given public health relevance and the potential for dissemination facilitated by mass gatherings[38]. Antimicrobial-resistant organisms (AROs) are also targets of expanded WES[39,40] with surveillance focused on the presence of specific ARGs of public health significance[41]. Monitoring has been established as a critical step in addressing the proliferation of AMR[42] with efforts having been made to test for the presence and level of ARGs at wastewater treatment facilities[39,43,44]. Exacerbating the threat of AMR are rainfall-driven combined sewer overflows (CSOs) and bypass events that can introduce partially treated effluent into receiving waters, increasing environmental ARG loads.

WES may be implemented through a OneHealth framework that considers the movement of organisms and resistance determinants between humans, infrastructure, and natural systems[45]. Wastewater is a critical connection between these systems and thus surveillance implemented here captures both human population dynamics and pathways for dissemination to the environment. Mass gatherings increase population density and can strain sanitation infrastructure. WES implemented during these events is

78 opportune for advancing knowledge of disease trajectories in human population and ARG
79 dissemination in the environment.

80 The 2024 NFL Draft was held in Detroit, MI from April 25-27, 2024, with events
81 concentrated in an area with an approximate radius of 1 km near the riverfront in downtown
82 Detroit. This event drew approximately 775,000 individuals to the city of Detroit[46,47] of which
83 an estimated 30% travelled more than 160 km to attend the event. Visitors to Detroit
84 included people from over 20 different nations and all 50 states, with some individuals
85 coming from as far afield as Australia[48]. Almost all of Detroit's 45,140 hotel rooms were
86 occupied for the Draft weekend, with spillover absorbed by neighbouring Windsor, ON, a
87 region separated from Detroit by a river and high-traffic international land border.

88 Here, we used the 2024 NFL Draft as a natural experiment to explore WES utility for
89 mass gatherings across two domains: (1) respiratory pathogens in wastewater; and (2)
90 public health relevant ARGs, with emphasis on carbapenemases, in wastewater and the
91 Detroit River, an environmental reservoir for wastewater treatment plant (WWTP) effluent.
92 We also compared multiplex RT-qPCR with a nanofluidic OpenArray® platform to assess
93 method agreement across matrices. We hypothesized that respiratory signals would not
94 increase immediately given the primarily outdoor nature, late-season timing of the event,
95 and its brevity (in comparison to the incubation of respiratory viruses). We also expected
96 that ARGs could show transient changes, and that heavy rainfall coincident with the Draft
97 could elevate environmental ARG detections due to CSO and/or bypass activity.

98 **Methods**

99 **Site information**

100 Sampling sites included five wastewater treatment facilities and a surface water
101 transect of the Detroit River with six sample collection sites (Figure 1). The Draft weekend
102 coincided with a wet weather period in the Windsor-Detroit region, with approximately 40
103 mm of rain falling over a 48 h period (Sunday-Tuesday)[49]. This influx of precipitation
104 contributed to CSO events where partially treated WWTP effluent and diluted raw sewage
105 was discharged into the Detroit River or its tributaries from both sides of the Canda-USA

border[50]. Wastewater treatment facilities were identified as potentially impacted by the NFL Draft or as control sites based on proximity (Table 1). Additional site information can be found in S1.

**Table 1.** Site characteristics and sample collection modalities

| Facility Name | Site ID | Location | Site type | Population served | Sample type | Sampling frequency | Role |
|---|---|---|---|---|---|---|---|
| Water Resource Recovery Facility (WRRF) | NIEA | Detroit, MI, USA | Interceptor feeding wastewater treatment plant | 1482000 | 1L 24h composite | 1×weekly. Daily sampling during Draft | Impacted site |
| | OAK | Detroit, MI, USA | Interceptor feeding wastewater treatment plant | 840600 | 1L 24h composite | 1×weekly Daily sampling during Draft | Impacted site |
| | JEFF | Detroit, MI, USA | Interceptor feeding wastewater treatment plant | 492000 | 1L 24h composite | 1×weekly Daily sampling during Draft | Impacted site |
| Anonymous Windsor-Essex Wastewater Treatment Plant | WEWTP | Windsor-Essex, ON, Canada | Wastewater treatment plant | 180000 | 1L 24h composite | 5×weekly Daily sampling during Draft | Impacted site |
| Leamington Pollution Control Centre | LPCC | Leamington, ON, Canada | Wastewater treatment plant | 18000 | 1L 24h composite | 3×weekly | Control site |
| Chatham Water Pollution Control Plant | CHWW | Chatham, ON, Canada | Wastewater treatment plant | 48000 | 0.5L 24h composite | 3×weekly | Control site |
| Atlantic Avenue Water Pollution Control Plant | TB | Thunder Bay, ON, Canada | Wastewater treatment plant | 97500 | 0.5L 24h composite | 3×weekly | Control site |
| Detroit River Transect | UP | Upstream of Detroit River outfall | Surface water | NA | 2L Grab | Event based | Env sample |
| | PO | Detroit River outfall | Surface water | NA | 2L Grab | Event based | Env sample |
| | DS1 | Downstream of Detroit River outfall | Surface water | NA | 2L Grab | Event based | Env sample |
| | DS2 | Downstream of Detroit River outfall | Surface water | NA | 2L Grab | Event based | Env sample |
| | DS3 | Downstream of Detroit River outfall | Surface water | NA | 2L Grab | Event based | Env sample |
| | DS4 | Downstream of Detroit River outfall | Surface water | NA | 2L Grab | Event based | Env sample |

## Sample collection

Untreated wastewater influent was collected from each of the wastewater treatment facilities included in the study at different weekly frequencies (Table 1) with daily sampling between April 24-29 from each of the three interceptors (NIEA, OAK, and JEFF) of the Great Lakes Water Authority Water Resource Recovery Facility (WRRF) as well as the WWTP plant (WEWTP) in Windsor, ON. All samples were transported directly to the laboratory in coolers on ice and processed upon arrival. Surface water grab samples (2 L) were collected in duplicate from each site in the Detroit River transect (Figure 1). Environmental samples were collected on April 25, prior to the 2024 NFL Draft, and on April 29 following the end of the he event.

**Figure 1.** Locations of sampling sites making up the Detroit River transect. Samples were collected on 2024-04-25, prior to the 2024 NFL Draft, and on 2024-04-29, after the event.

126 **Sample processing**

127 Influent samples collected from WWTPs were concentrated by filtering between 60-
128 120 mL through 0.22 µm Sterivex PES cartridge filters (MilliporeSigma, Burlington, MA).
129 River water samples were likewise concentrated by passing 500-800 mL of water through
130 cartridge filters. Immediately following filtration, the filters were sealed and flash-frozen
131 through immersion in liquid nitrogen, with filters stored at -80°C before nucleic acid
132 extraction. Total nucleic acids were extracted from filters using the AllPrep PowerViral
133 DNA/RNA kit (Qiagen, Germantown, MD) with the addition of 5% (v/v) 2-mercaptoethanol
134 to the lysis buffer. Nucleic acids were eluted in 50 µL of RNAse-free water. Samples were
135 not treated with DNase upon extraction. Extracted nucleic acids were stored in LoBind
136 tubes at -80°C.

137 **RT-qPCR assays for quantification of respiratory viruses and carbapenemase genes**

138 Respiratory viruses, select carbapenemase genes and Pepper Mild Mottle Virus
139 (PMMoV) were quantified using established RT-qPCR assays. Severe Acute Respiratory
140 Syndrome Coronavirus 2 (SARS-CoV-2), influenza A virus (IAV), influenza B virus (IBV), and
141 respiratory syncytial virus (RSV) were the respiratory viruses measured. PMMoV, a human
142 fecal indicator[51] and established wastewater surveillance normalizing agent[52], was used to
143 normalize the wastewater signal for targets measured using RT-qPCR assays.
144 Carbapenemase genes, including $bla_{KPC}$, $bla_{NDM}$, $bla_{OXA-48}$, $bla_{VIM}$, and $bla_{VIM7}$ were measured
145 using two multiplexed assays[44]. All targets were measured in at least technical triplicate.
146 Standard curves were generated using serial dilution of synthetic RNA or DNA controls.
147 Inhibition was assessed using an internal amplification control, and template RNA was
148 diluted to overcome inhibition. Negative controls were included with each RT-qPCR run.
149 Detailed RT-qPCR methods are described in S2.

150

151 **Development of the nanofluidic qPCR card using TaqMan® assays in the OpenArray ®**
152 **platform**

153 Assays for the quantification of clinically important and locally relevant ARGs and
154 genes associated with mobile genetic elements (MGEs) were selected for inclusion on the
155 OpenArray® card (Table 2). The OpenArray® card also included assays for 16S rRNA and
156 crAssphage to allow normalization and act as controls. Assays were selected from the
157 literature and optimized for TaqMan chemistry. The resulting nanofluidic RT-qPCR card was
158 used to analyze samples in technical duplicate in 33nL reactions on a Quant Studio 12K
159 Flex Real-Time PCR System (Thermo Fisher Scientific, Waltham, MA). A 7-point standard
160 curve, created through a serial dilution of pooled gBlocks™ (Integrated DNA Technologies,
161 Coralville, IA), was run on each OpenArray ® plate. Assay performance met established
162 technical standards for RT-qPCR. Full assay design and nanofluidic qPCR methods can be
163 found in S3.1 and S3.2.

164 **Table 2.** Antimicrobial resistance genes monitored, associated drug resistance, and rationale for inclusion on
165 the Nanofluidic qRT-PCR chip

| Class of antimicrobial | Gene(s) | Rationale for testing |
|---|---|---|
| Aminoglycoside | *aph(3')-Ia, aac(6')-Ib-cr* | Often used in pediatric settings[53] Renewal in interest with rise in AMR for treatment of MDR infections[54]. Most common resistance mechanism for aminoglycosides is through enzymatic modification with the listed ARGs coding for the most common enzymes[55] |
| Carbapenems | $bla_{KPC}$, $bla_{NDM}$, $bla_{OXA-48}$, $bla_{IMP}$, $bla_{VIM}$ | Rapid spread and ability to infect patients in healthcare settings. Rise in prevalence with few viable treatment options. Often resistant to multiple classes of antibiotic [56–58]. |
| Cephalosporins/extended spectrum ß-lactam (ESBL) antibiotics | $bla_{CMY-2}$, $bla_{SHV}$, $bla_{TEM}$, *CTX-M1, CTX-M9,* | Beta-lactams are highly common treatments for bacterial infections but resistance levels are high[59]. Some later generation cephalosporins and ESBL are considered last resort antibiotics[60]. Levels of cephalosporin resistance are generally rising[61]. Identified as likely a large threat to human health with emerging concerns regarding environmental spread[62]. |
| Colistin | *mcr-1* | Listed as a reserve antimicrobial agent for last resort use by the World Health Organization[63]. Rapid global spread[42]. |
| Fluoroquinolones | *gyrA83L-Esh, QnrB1, qnrS* | Widely used theraputics[64] with fluoroquinolone resistant infections resulting in worse patient outcomes and increase risk of mortality[65]. Resistance is widespread[66–69]. Many fluoroquinolones are on the WHO "Watch" list. [63] |
| Glycopeptides (vancomycin) | *vanA* | Last resort antibiotic used in the treatment of serious gram-positive bacterial infections[70,71]. Recent rapid increases in resistance [72] Vancomycin is on the WHO "Watch" list. [63] |

| | | |
|---|---|---|
| Macrolides | *mphA* | Used widely in the treatment of common infections such as pneumonia, sinusitis, and chlamydia. Members include erythromycin, clarithromycin, azithromycin[73]. Associated with mobility[74] *mphA* is plasmid associated and mobile with evidence of transmission through horizontal gene transfer[75]. Commonly prescribed throughout Ontario[76] |
| Methicillin | *mecA* | Primary gene associated with beta-lactam resistance in Methicillin-Resistant Staphylococcus aureus (MRSA)[77] Thought to be mobile and has been shown confer advantages to bacterial exposed to a diversity of antimicrobial agents/chemical environments[78] |
| Tetracycline | *tetA, tetM* | Broadly administered in agriculture and human healthcare[62]. Evidence of co-selection with fluoroquinolone resistance genes[79] |
| Sulfonamides | *sul1, sul2* | Widely used and well established class of antimicrobial agent[42]. Broad spectrum antibiotics with both human and agricultural applications[80]. |
| Trimethoprim | *dfrA1* | Antimicrobial agent often used in the treatment of urinary tract infections. Widely prescribed in Ontario[76]. |
| Associated with resistance to multiple therapeutics | *cfr, int1* | The *cfr* gene is associated with multi-drug resistance[81] while the *int1* gene is a sign of the presence of mobile genetic elements often associated with AMR. Presence of *int1* alone does not indicate AMR. However, it is associated with multiple ARGs and their mobility[82,83] |
| Normalization/Control | 16S rRNA, CrAssphage | crAssphage is a bacteriophage found in association with human waste making it a good fecal indicator and a measure of wastewater concentration that can be used for normalization of wastewater signals [84,85].<br>A general assay for 16S rRNA was also incorporated to act as a control and for normalization. |

## Statistical methods

Data analysis was performed in R (version 4.5.1)[86] with data manipulation and visualization relying on the *tidyverse* suite of packages[87]. Multiple different measurement techniques were employed in this investigation, leading to the creation of five distinct datasets. Statistical analyses were conducted separately for each dataset due to differences in sampling frequency, sample matrix, availability of covariate data, data distribution, and response variable. All analyses tested changes in wastewater and environmental occurrence of pathogens associated with the mass gathering of 2024 NFL Draft attendees and the co-occurring CSO event.

177 **Interrupted time series (ITS) analysis**

178 To test if the 2024 NFL Draft coincided with altered concentrations of respiratory
179 pathogens or carbapenemase genes in wastewater, we fit Generalized Linear Mixed Models
180 (GLMMs) using the *glmmTMB* package. Independent analyses were conducted on
181 "affected" and "control" sites for a quasi-experimental design. Model specification
182 followed a segmented regression framework with a binary "event" variable (modelling
183 immediate event-related changes) and a "post-time" variable (more gradual event-related
184 changes). Models controlled for a variety of covariates (pH, temperature, flow,
185 precipitation, etc.) and temporal autocorrelation was addressed via an autoregressive term
186 for all targets and seasonal harmonics for respiratory virus response variables. A Tweedie
187 distribution with a log link was used for continuous zero-inflated viral pathogen
188 concentration data. A Gamma distribution with a log link was used for individual
189 carbapenemase gene concentration data, while a Tweedie distribution was used for the
190 composite measure of all assayed carbapenemase genes. To account for multiple testing,
191 p-values were adjusted using the Benjamini-Hochberg (BH) False Discovery Rate (FDR)
192 method. Adjustment was performed independently for respiratory viruses and
193 carbapenemase genes and for "control" and "affected" sites. Details can be found in S4.1
194 and S4.2.

195 **Multivariate resistome characterization**

196 The Open Array nanofluidic RT-qPCR card was used to measure a subset of samples
197 collected from WWTPs during the month surrounding the 2024 NFL Draft. ARG
198 concentrations were normalized to the concentration of crAssphage and subjected to
199 fourth root transformation. Data was split into the uneven groups ("before", "during" and
200 "after") relative to the timing of the 2024 NFL Draft. Characterization of the resistome was
201 carried out with Non-Metric Multidimensional Scaling (NMDS) using Bray-Curtis
202 dissimilarity matrices. A marginal Permutational Multivariate Analysis of Variance
203 (PERMANOVA) was then run on the data to partition sources of variation, and a distance-
204 based redundancy analysis was used for visualization of variance partitioning. A

205 Permutational Analysis of Multivariate Dispersions (PERMDISP) was used to test if
206 observed differences arose from differences in resistome or within-group variance. A
207 principal component analysis (PCA) was run to identify ARGs driving variability. Finally, JEFF
208 was analyzed alone as it drains the NFL Draft location. A Kruskal-Wallis test was used to
209 determine if concentration differences existed between the "before", "during" and "after"
210 groupings for the measured ARGs. The p-values were adjusted for multiple comparisons
211 using the Benjamini-Hochberg method. Details can be found in S4.3.

212 **Environmental detection**

213 To determine if the CSO events altered the occurrence of carbapenemase genes in
214 the Detroit River, detection frequencies were calculated for each carbapenemase gene in
215 the pre- and post- CSO transects. Fisher's exact test was used to compare the detection
216 frequency. Additionally, a paired Wilcoxon signed-rank test was performed to evaluate
217 concentration changes for PMMoV normalized $bla_{KPC}$ between the pre- and post CSO
218 samplings.

219 To determine if the CSO and mass gathering event led to either changes in
220 abundance or detection frequency for additional ARGs, data produced by the Open Array
221 nanofluidic RT-qPCR card were employed. Data were normalized to 16S rRNA
222 concentrations and log-transformed before quantitative analysis. Detection frequencies
223 were also calculated for both the pre- and post- CSO groupings. Changes to detection
224 frequency were assessed using a GLMM with a binomial distribution and logit link function.
225 To prevent complete separation, ARGs that were constitutively detected or undetected in
226 either the pre-CSO or post-CSO grouping were excluded from logistic regression. The main
227 GLMM included ARG identity, sampling group (pre/post CSO) and the interaction of the two
228 as fixed effects. Random intercepts and slopes for groups nested within sites were also
229 included to account for differences between sites. Post-hoc comparisons were conducted
230 using estimated marginal means. A second GLMM was conducted with site and sample
231 grouping as fixed effects and gene as a random intercept to directly investigate site
232 heterogeneity. Quantitative abundance differences between pre- and post-CSO sample

233 groupings were tested using paired Wilcoxon signed rank tests with pairings assigned by
234 site identity and ARG. A sensitivity analysis was performed to identify the influence of
235 potential detection saturation in samples collected at a known WWTP outlet. To account
236 for multiple comparisons, p-values were adjusted using the Benjamini-Hochberg method
237 to control FDR. Model diagnostics were assessed using simulated residuals in the *DHARMa*
238 package. Details can be found in S4.4 and S4.5.

239 **Method comparison**

240 OpenArray® assays were compared with established RT-qPCR assays using a subset
241 of wastewater and environmental samples that were analyzed by both methods (n=42).
242 Comparison was limited to assays for $bla_{KPC}$, $bla_{NDM}$, and $bla_{OXA-48}$ as they were shared
243 between the OpenArray® and the multiplexed RT-qPCR assays. Qualitative agreement was
244 evaluated using Cohen's Kappa and detection frequency comparisons. Quantitative
245 agreement was determined through Bland-Altman analysis to calculate 95% limits of
246 agreement (LoA). Additional quantitative measures of method comparison included
247 Passing-Bablok regression, Deming regression, spearman correlation, Pearson correlation
248 and calculation of concordance correlation coefficients (CCC). Details can be found in
249 S4.6.

250 **Results**

251 **Respiratory pathogen dynamics**

252 ITS analysis showed no event-associated increase in wastewater concentrations of
253 SARS-CoV-2, IAV, IBV, or RSV at monitored sites. IBV showed a post-event decline (β=-
254 0.356, SE=0.143, p= 0.035), consistent with seasonal-tapering rather than event impact
255 (Figure 2). Variability in respiratory virus concentrations in wastewater was driven by
256 dilution and seasonality. Concentrations of SARS-CoV-2 were negatively associated with
257 flow (β=–0.288, SE=0.115, p = 0.035) and positively associated with PMMoV concentration
258 (β = 0.379; SE=0.065, p < 0.001), consistent with dilution. Likewise, IAV concentration in
259 wastewater was negatively predicted by flow (β=-0.467, SE=0.160, p = 0.012), consistent
260 with dilution. However, IAV concentrations were positively predicted by precipitation

(β=0.317, SE=0.079, p<0.001). RSV concentrations were positively associated with PMMoV (β= 0.455, SE= 0. 141, p = 0.005) while IAV was a negative predictor (β= -0.318, SE= 0.128 p = 0.035). Precipitation was positively associated with IBV concentration (β=0.345, SE=0.138, p = 0.035) while flow was negatively associated (β=-0.924, SE=0.284, p = 0.005). Finally, IBV was found to be positively associated with IAV concentration (β=0.814, SE=0.244, p = 0.004).

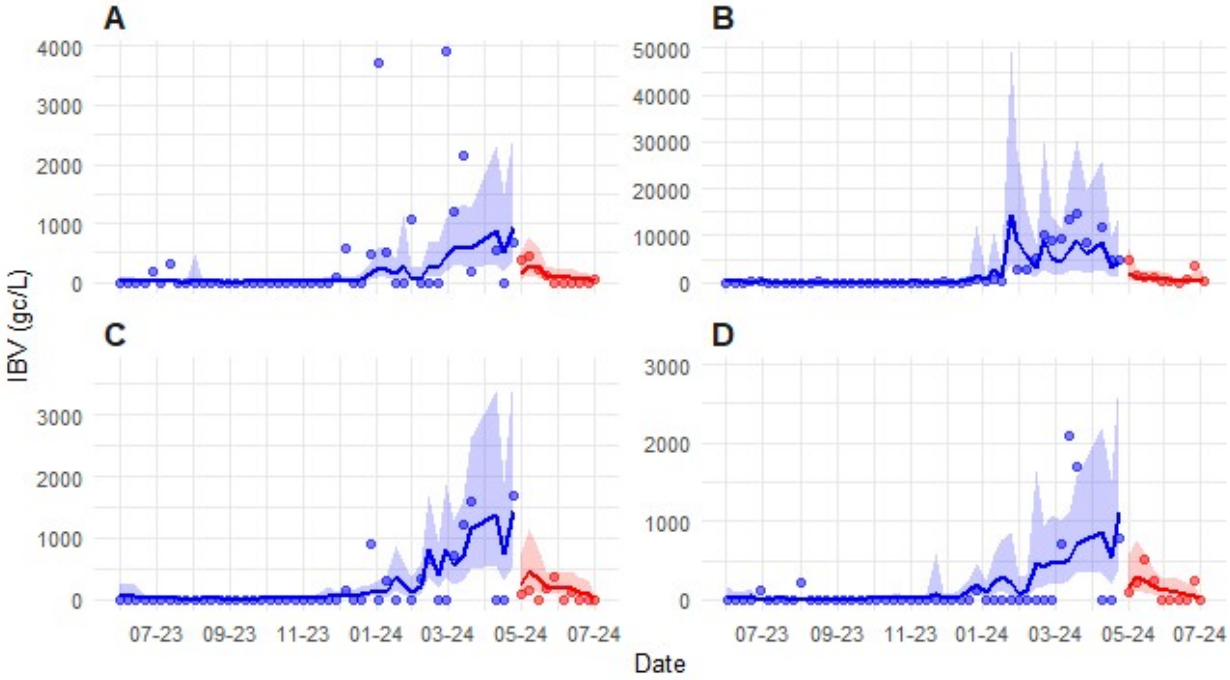


**Figure 2.** Longitudinal wastewater surveillance data for IBV at the four draft proximal sites (**A -JEFF** , **B-WEWTP, C-NIEA, D-OAK**) both before (blue), and after (red) the 2024 NFL Draft. Points represent IBV concentrations in gene copies per litre. Solid lines and shaded areas denote predicted mean concentrations and 95% confidence intervals.

Parallel analysis at control sites showed no event effects. The GLMM run for SARS-CoV-2 did not detect any stepwise increase in SARS-CoV-2 concentration or change in trend associated with the Draft. However, LRT indicated that the inclusion of “event” and “post time” parameters improved model fit (Table S10). Sensitivity analysis and visualization of the data indicate that this is due to noise in the N2 concentration at TB (Figure 3, Table 3).

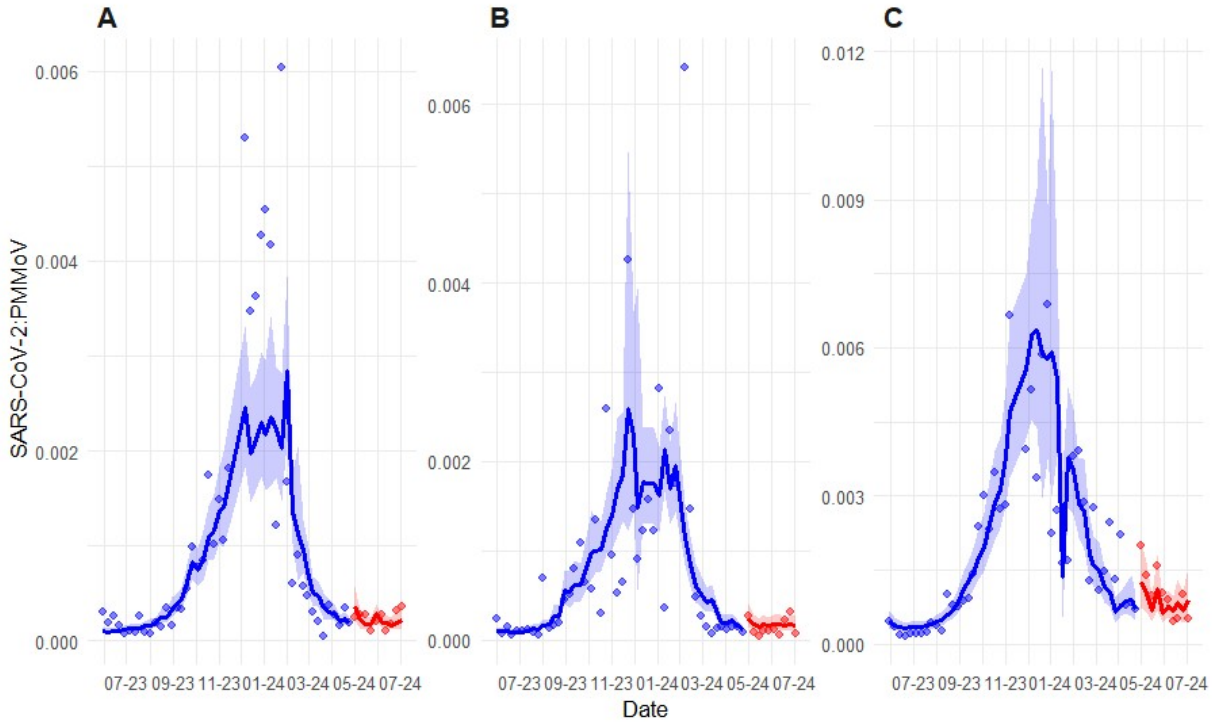


**Figure 3.** Longitudinal wastewater surveillance data for SARS-CoV-2 at the three control sites (**A -CHWW**, **B-LPCC, C-TB**) both before (blue), and after (red) the 2024 NFL Draft. Points represent mean N1 and N2 gene concentrations normalized to Pepper Mild Mottle Virus (PMMoV) concentration. Solid lines and shaded areas denote predicted mean concentrations and 95% confidence intervals, respectively, derived from a Generalized Linear Mixed Model (GLMM).

The detection of a marginal, site-specific fluctuation at a control location demonstrates sensitivity to minor background variance in the approach, reinforcing the validity of the null results observed at affected site cluster. This contrast confirms that while the modelling framework can identify localized shifts, no such signal was generated by the mass gathering event.

**Table 3.** Summary of Interrupted Time Series (ITS) model parameters, Likelihood Ratio Tests (LRT), and diagnostic checks for gamma GLMMS for N1 and N2 gene targets in the control site cluster.

| | | Target | |
|---|---|---|---|
| Metric | Statistic | N1 | N2 |
| Model Estimates | Event | 0.333 (p=0.272) | 0.393 (p=0.179) |
| | Post Time | 0.012 (p=0.789) | 0.025 (p=0.572) |
| Model Fit | ΔAIC | -0.5 | -4.0 |
| | Log-Likelihood | 1122.1 | 1136.4 |
| | Dispersion | 0.187 | 0.193 |
| LRT | Chi-Square | 4.485 | 8.066 |
| | p-value | 0.106 | 0.018* |
| DHARMa diagnostics | KS | p=0.309 | P=0.627 |
| | Dispersion | p=0.892 | P=0.424 |
| | Quantiles | p=0.074 | P=0.069 |
| | Outlier | P=0.288 | P=0.288 |

## Carbapenemase gene concentration in wastewater

ITS analysis indicated a statistically significant increase in the composite measure of carbapenemase gene concentrations concurrent with the 2024 NFL Draft (β=0.625, SE=0.290, p=0.031). An ~87% increase in combined ARG burden could be observed following the Draft weekend (Figure 4).

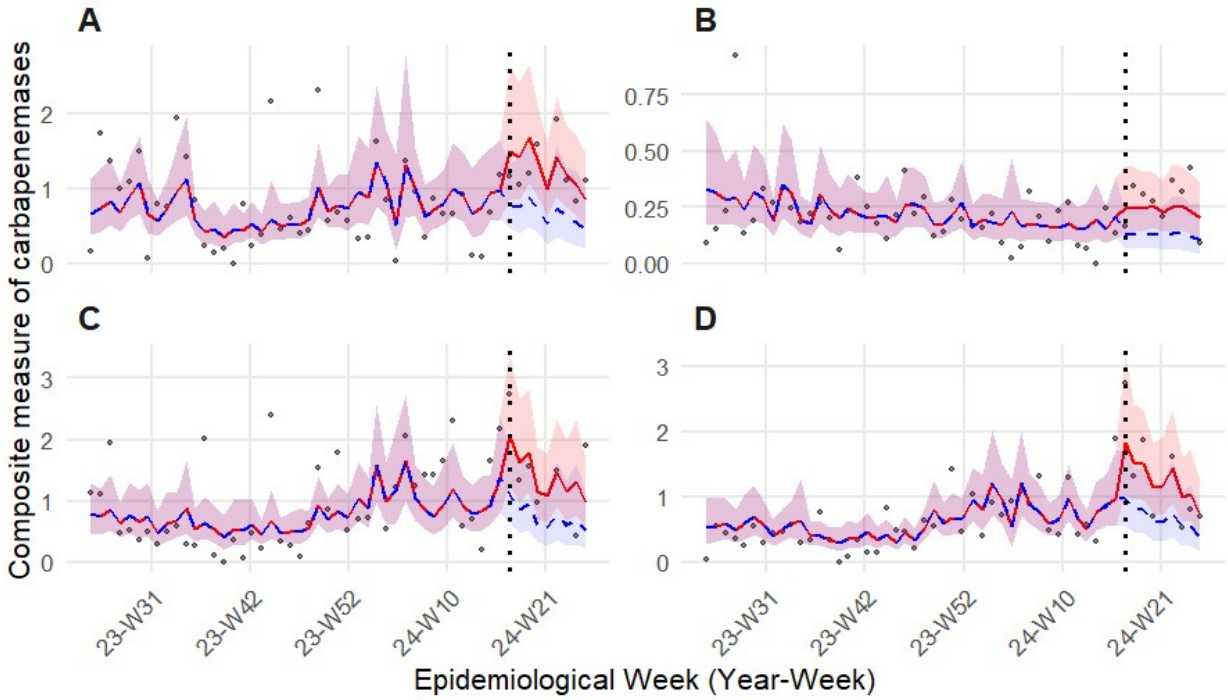


**Figure 4.** Longitudinal wastewater surveillance data for a composite measure of carbapenemase gene concentrations at the four Draft proximal sites (**A -JEFF** , **B-WEWTP, C-NIEA, D-OAK**) both before, and after the 2024 NFL Draft (vertical dotted line). Points represent a composite carbapenemase index calculated by taking the mean of z-score standardized normalized gene concentrations *for* $bla_{KPC}$, $bla_{NDM}$, $bla_{OXA48}$, $bla_{VIM}$, and $bla_{VIM7}$. The redline and shading represent model predicted factual fit and 95% confidence intervals. The dashed blue line and shading represent the counter factual scenario (model predictions excluding draft related parameters).

However, the event did not lead to a change in the trend for the ARG composite index as the post-event temporal trend variable was non-significant (p = 0.96). ITS for individual carbapenemase genes revealed that the increase was primarily driven by a spike in normalized wastewater concentration for $bla_{OXA-48}$ (β=1.38, SE=0.374, p=0.006), which increased by ~400% following the Draft (Figure 5). A parallel increase in $bla_{KPC}$ concentration (β=0.447, SE=0.212, p=0.035) did not survive FDR correction (p=0.18). ITS for $bla_{NDM}$, $bla_{VIM}$, and $bla_{VIM7}$ indicate that the 2024 NFL Draft did not significantly impact normalized ARG concentration despite event estimates all indicating post-event increases.

Flow was a significant positive predictor of ARG concentration across 4 of 5 gene targets (Table S14). Higher flows were consistently associated with increased normalized ARG concentrations.

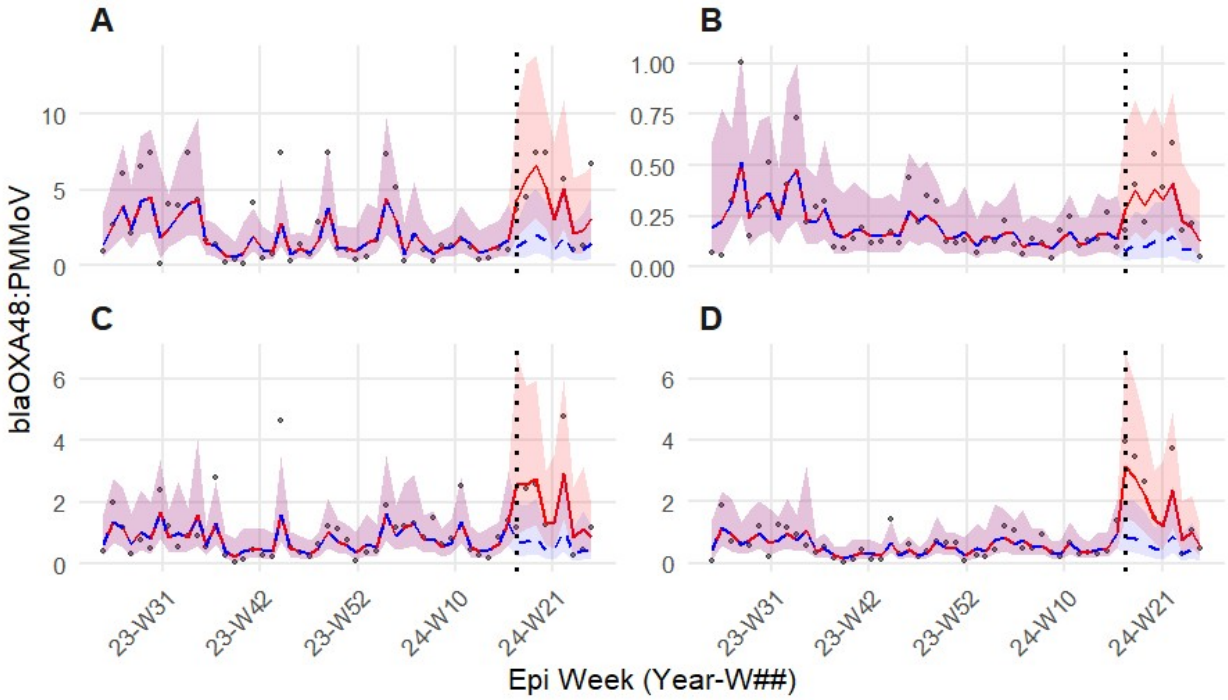


**Figure 5.** Longitudinal wastewater surveillance data for PMMoV normalized $bla_{OXA-48}$ concentrations at the four Draft proximal sites (**A -JEFF** , **B-WEWTP, C-NIEA, D-OAK**) both before, and after the 2024 NFL Draft (vertical dotted line). Points represent normalized wastewater concentrations. The redline and shading represent model predicted factual fit and 95% confidence intervals. The dashed blue line and shading represent the counter factual scenario (model predictions excluding draft related parameters).

## Resistome variability

Characterization of the resistome with NMDS revealed samples collected from the same site clustered regardless of sample collection time in relation to the 2024 NFL Draft stress= 0.068; Figure 6).

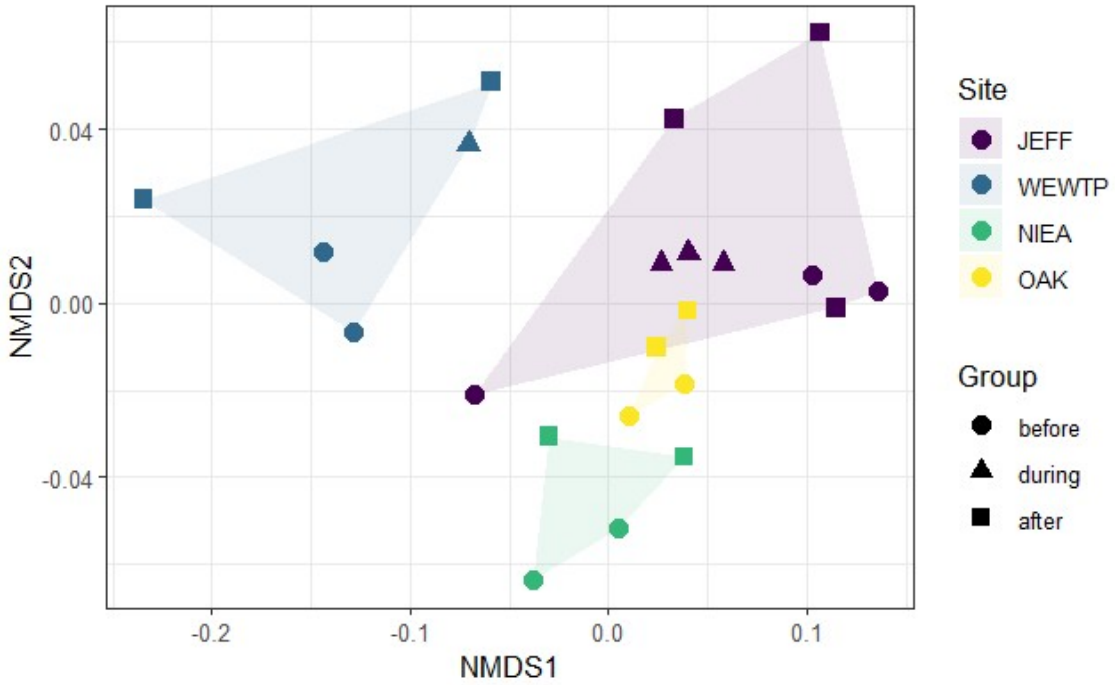


**Figure 6.** Resistome structure across collection sites and draft periods. Non-metric Multidimensional Scaling (NMDS) ordination based on Bray-Curtis dissimilarities of crAssphage normalized antimicrobial resistance gene concentrations. Shaded areas represent site-specific clusters. Points are colored by site identity and shaped by draft period (before, during, and after). The low stress value (0.068) indicates a good representation of resistome in two-dimensional space.

The marginal PERMANOVA corroborated the NMDS visualization, indicating that site identity explained 61% of variance in resistome ($R^2 = 0.611$, $F_{3,16} = 9.30$, $p = 0.001$) while collection period was statistically insignificant ($R^2 = 0.033$, $F_{2,16} = 0.76$, $p = 0.531$) (Table 4).

**Table 4.** Multivariate analysis of resistome composition. Results of the marginal Permutational Multivariate Analysis of Variance (PERMANOVA) based on Bray-Curtis dissimilarities. Site identity serves as the primary driver of community variance, while the NFL Draft period (Group) did not significantly influence the resistome structure

| Factor | Degrees of Freedom | $R^2$ | F-Statistic | p-value |
|---|---|---|---|---|
| Site | 3 | 0.611 | 9.305 | 0.001 |
| Draft period | 2 | 0.033 | 0.760 | 0.531 |
| Residual | 16 | 0.350 | - | - |
| Total | 21 | 1 | - | - |

**Note:** Site dispersion ($p = 0.236$) and Group dispersion ($p = 0.421$) were non-significant, supporting the PERMANOVA findings.

The PERMDISP showed that these differences were not a result of heterogeneity of variance with no difference in dispersion between groups ($F_{2,19} = 0.90$, $p = 0.421$) or site identities ($F_{3,18} = 1.55$, $p = 0.236$). The first two principal components of the PCA accounted for 78% of the variance. The highest loadings for PC1 were *int1*, *sul1*, *aac(6')-Ib-cr*, *tet(A)*,

*sul2*, *mphA, qnrs*, *dfrA1*, $bla_{OXA-48}$, and $bla_{TEM}$. The top PC1 loadings had the same sign, indicating the top contributors varied together across collection sites (Figure 7). The Kruskal-Wallis test for JEFF revealed no significant difference in concentration for any ARG in the "before", "during", or "after" groups.

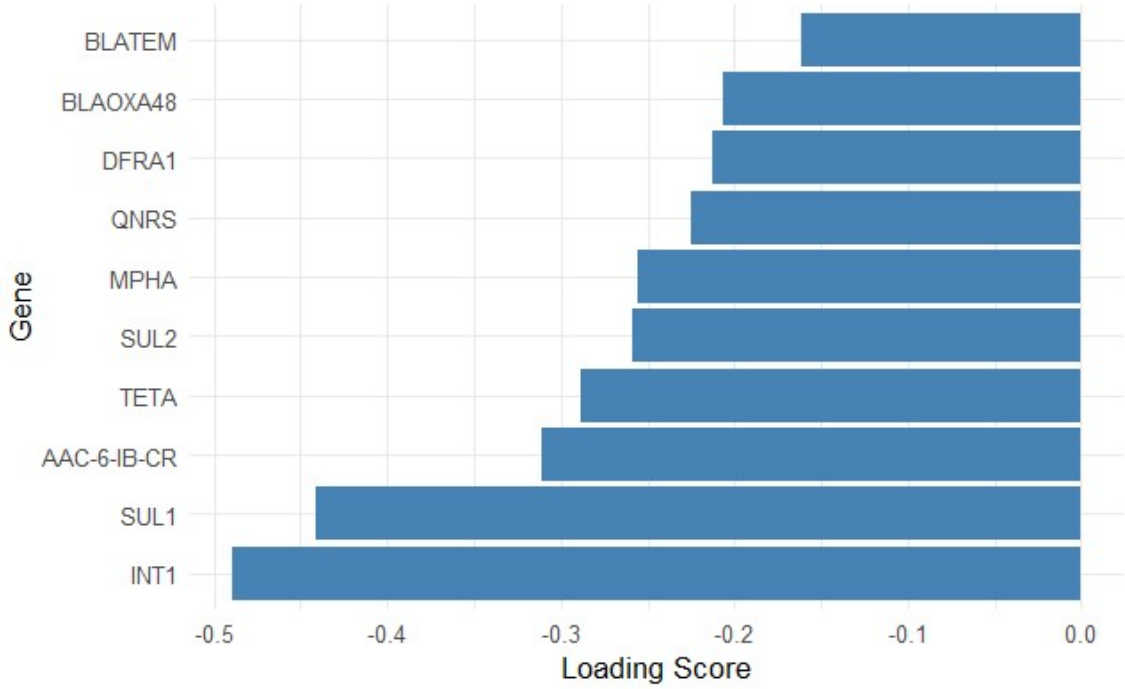


**Figure 7.** Loading scores for the top 10 antimicrobial resistance genes (ARGs) contributing to the first principal component (PC1). PC1 accounted for a significant portion of the total variance in the dataset. All top-loading genes share the same directional sign, indicating that these ARGs vary synchronously across the sampled locations.

## Environmental dissemination of ARGs

Detection frequencies for $bla_{KPC}$, $bla_{OXA-48}$ and $bla_{VIM7}$ rose nominally in the post-Draft transect. However, detection frequency increases were non-significant for all carbapenemase genes. A paired Wilcoxon signed-rank test for PMMoV normalized $bla_{KPC}$ indicated an increased median concentration between the pre- and post CSO samplings ($V = 614$, $p<0.001$). Heterogeneity in effect could be observed between sites (Table 5, Figure 8).

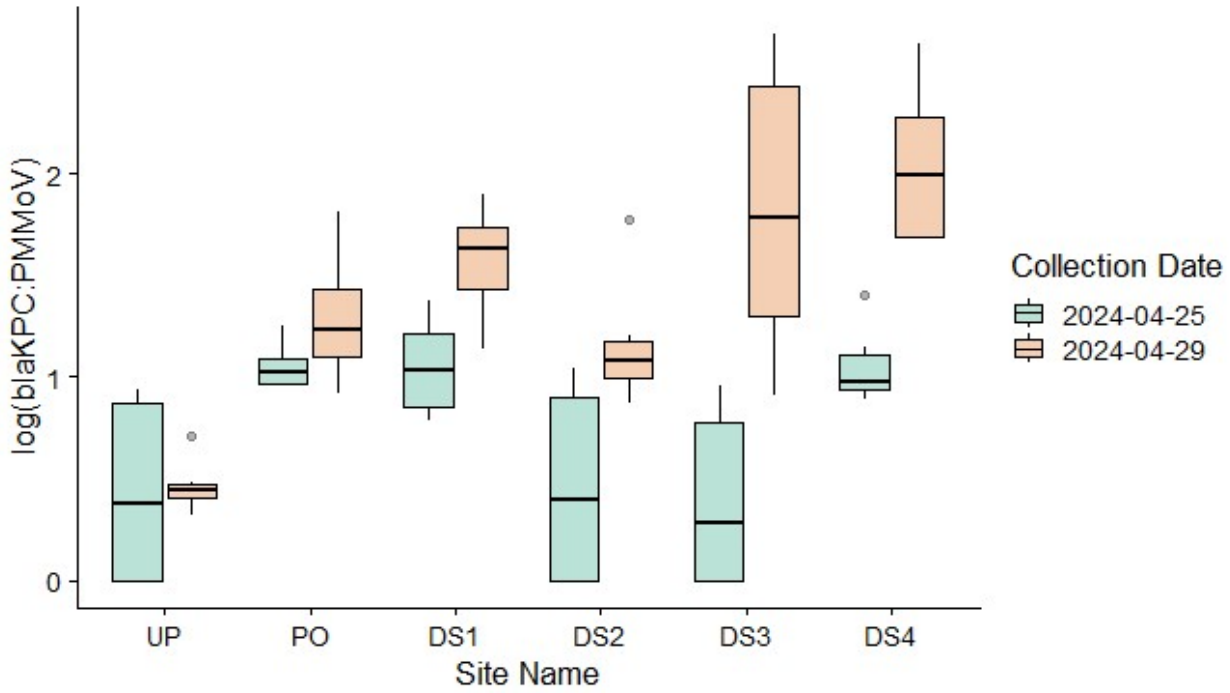


**Figure 8.** Log PMMoV normalized $bla_{KPC}$ concentrations before and after the 2024 NFL Draft and combined sewer overflow (CSO) at six sites in the Detroit River. Sites are arranged geographically along the x-axis.

Detection frequencies were also calculated for ARGs included on the OpenArray® for both the pre- and post- CSO groupings. Detection frequency increased following the Draft weekend for 62.5% of ARGs assayed (Figure 9).

**Table 5.** Median log PMMoV normalized $bla_{KPC}$ concentrations for each environmental sampling site before and after the 2024 NFL Draft and associated combined sewer overflow (CSO) event. The mean difference represents the magnitude of the concentration shift. P-values were calculated using site-specific paired Wilcoxon signed-rank tests

| Site | Median before | Median after | Mean difference | Wilcox p-value | Significance |
|---|---|---|---|---|---|
| DS1 | 1.030 | 1.631 | 0.522 | 0.031 | Significant |
| DS2 | 0.394 | 1.077 | 0.699 | 0.156 | Non-significant |
| DS3 | 0.286 | 1.787 | 1.429 | 0.031 | Significant |
| DS4 | 0.976 | 1.991 | 0.987 | 0.031 | Significant |
| PO | 1.023 | 1.233 | 0.238 | 0.094 | Non-significant |
| UP | 0.375 | 0.443 | 0.035 | 0.844 | Non-significant |

The binomial GLMM showed that sample collection timing had a significant effect on the probability of *crAssphage* detection (Estimate = 11.46, p = 0.0008), suggesting that the 2024 NFL Draft and CSO greatly increased detection probability. Additionally, the fitted model had high levels of variance for the random intercept ($\sigma^2$ = 62.07, SD=7.88) and the

random slope for the "after" group ($\sigma^2$ =6.36, SD=2.52), indicating large differences in baseline detection probabilities and Draft effect between sites. Interaction terms between ARG and sampling group were not statistically significant, indicating that the relative magnitude of the post-Draft increase did not differ significantly among genes. Post-hoc pairwise comparisons for each gene included in the model found that detection probability increased for 6 genes including: *crAssphage, AAC(6')-lb-cr, qnRS, tetA, mph(A),* and $bla_{KPC}$. (Table S26). Increased detection probability post-Draft was corroborated by the paired Wilcoxon signed-rank test. Ten ARGs displayed statistically significant increases in concentration following the event, with no ARGs showing a significant decrease in abundance (Table S29).

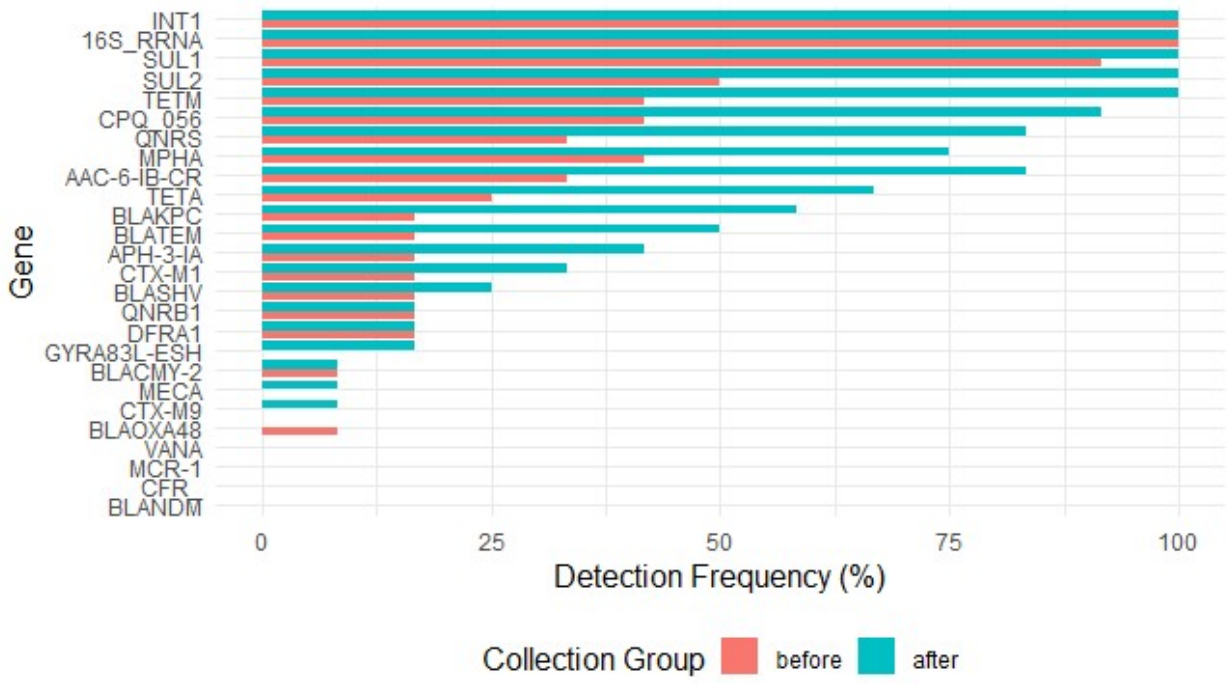


**Figure 9.** Detection frequences for ARGs in the Detroit River before and after the 2024 NFL Draft and combined sewer overflow event. Horizontal bars represent the percentage of samples positive for each genetic target before (red) and after (teal) the CSO event.

The GLMM investigating site heterogeneity identified PO as the site with the highest detection probability, consistent with a point source of pollution (Table S30). An additional 4 ARGs showed statistically significant increases in concentration when the PO site was removed from the Wilcoxon signed-rank test (Table S33), suggesting that constitutively high

ARG concentration at PO was masking significant increases in ARG concentration at other sites (Figure 10).

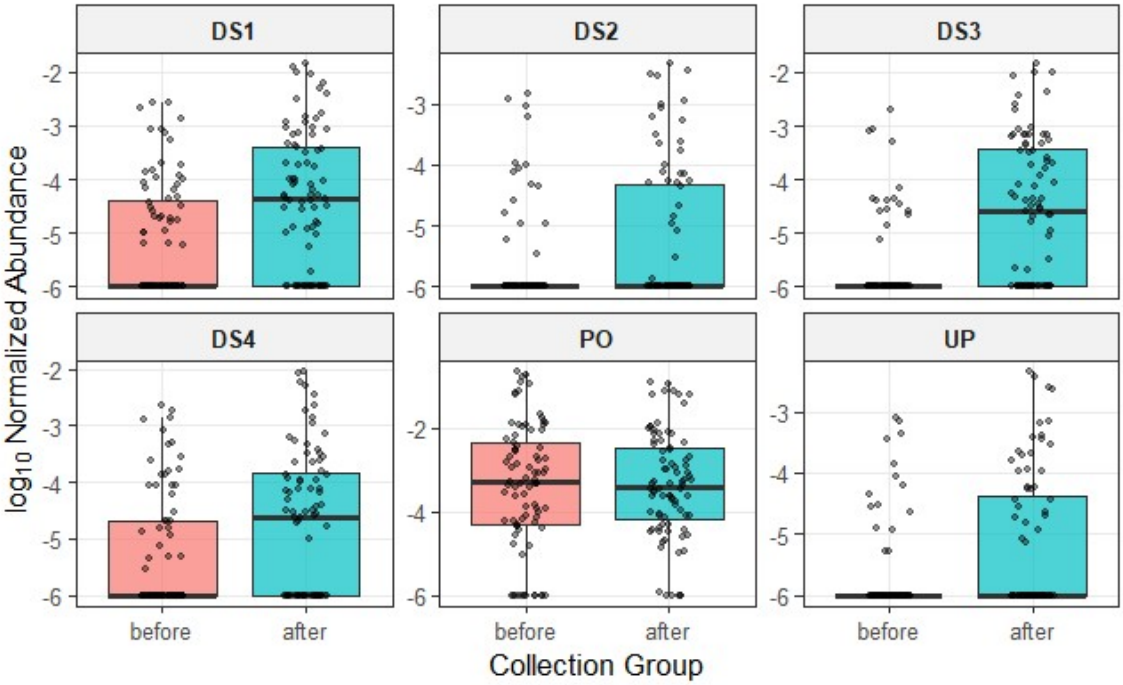


**Figure 10.** Log 16S rRNA normalized ARG abundances at six sites in the Detroit River before and after the 2024 NFL Draft and CSO event. Box plots represent the median and interquartile range of Log 16S rRNA normalized ARG concentrations with individual measurements over laid as a jitter. Facets represent each sampling site (DS1–DS4, PO, and UP). All sites save for PO show an increase in ARG abundance following the CSO.

**Method comparison**

In wastewater, detection was 100% for all targets shared across platforms. In environmental samples, OpenArray showed lower sensitivity, missing low abundance targets detected by RT-qPCR (Table 6). Bland-Altman analysis showed that $bla_{KPC}$ had the narrowest LoA with $bla_{NDM}$ and $bla_{OXA\text{-}48}$ having wider LoAs (Figure S19). Both $bla_{KPC}$ and $bla_{NDM}$ had positive bias while $bla_{OXA\text{-}48}$ showed negative bias. Fold change analysis showed similar results, with the OpenArray having higher measurements in wastewater samples for $bla_{KPC}$ and $bla_{NDM}$ but lower for *blaOXA-48* (Figure S20).

412 **Table 6.** Comparison of RT-qPCR and nanofluidic RT-qPCR performance for detection of select antimicrobial
413 resistance genes (ARGs) in different sample matrices

| Target | Matrix | No. Observations | RT-qPCR Positive | OpenArray Positive | Detection Gap | Kappa (κ) | p-value |
|---|---|---|---|---|---|---|---|
| $bla_{KPC}$ | Global | 42 | 42 (100%) | 31 (73.8%) | -26.20% | 0.000* | NA |
| | Wastewater | 18 | 18 (100%) | 18 (100%) | 0% | 1.000** | NA |
| | Environmental | 24 | 24 (100%) | 13 (54.2%) | -45.80% | 0.000* | NA |
| $bla_{NDM}$ | Global | 42 | 34 (81.0%) | 18 (42.9%) | -38.10% | 0.300 | 0.006 |
| | Wastewater | 18 | 18 (100%) | 18 (100%) | 0% | 1.000** | NA |
| | Environmental | 24 | 16 (66.7%) | 0 (0.0%) | -66.70% | 0.000* | NA |
| $bla_{OXA-48}$ | Global | 42 | 26 (61.9%) | 25 (59.5%) | -2.40% | 0.751 | < 0.001 |
| | Wastewater | 18 | 18 (100%) | 18 (100%) | 0% | 1.000** | NA |
| | Environmental | 24 | 8 (33.3%) | 7 (29.2%) | -4.10% | 0.516 | 0.011 |

414
415 The strength of monotonic agreement between the results of the OpenArray and RT-
416 qPCR varied by target with the strongest agreement for $bla_{KPC}$ and weakest for $bla_{OXA-48}$
417 (Table 7). Pasing-Pablok and Demming regression revealed proportional bias for all targets
418 (slopes >1.0), and large negative intercepts (Table S34). This pattern indicates a relative
419 underestimation of ARG concentrations by the OpenArray® at lower analyte
420 concentrations, transitioning to a relative overestimation at higher analyte concentrations.
421 CCC was the highest for $bla_{KPC}$ (CCC=0.94) and lower for $bla_{NDM}$ (CCC = 0.88) and $bla_{OXA-48}$
422 (CCC=0.75) (Table 7). Only $bla_{KPC}$ demonstrated substantial methodological agreement
423 between platforms based on previously determined criteria[88].

424 **Table 7.** Correlation and agreement of measurements for select ARGs assayed with RT-qPCR assays and
425 nanofluidic RT-qPCR

| Target | n | Spearman | Pearson | CCC (95% CI) | Mean Bias (log) | LoA (95%) |
|---|---|---|---|---|---|---|
| $bla_{KPC}$ | 16 | 0.91 | 0.97 | 0.94 (0.74–0.97) | 0.15 | -0.21 to 0.51 |
| $bla_{NDM}$ | 15 | 0.77 | 0.93 | 0.88 (0.69–0.94) | 0.29 | -0.77 to 1.34 |
| $bla_{OXA-48}$ | 18 | 0.64 | 0.82 | 0.75 (0.42–0.86) | -0.27 | -1.11 to 0.58 |

426

427 **Discussion**

428 This study supports the utility of WES for monitoring and assessing the impact of
429 mass gatherings on the spread of viral pathogens and antibiotic resistance genes. The 2024
430 NFL Draft served as a natural experiment. We measured the concentrations of public
431 health relevant ARGs and seasonal respiratory pathogens in wastewater and in the Detroit
432 River, which receives treated effluent from the Detroit-Windsor metropolitan region. WES
433 detected no surge in respiratory viruses associated with the event, yet identified a

434 transient, event-coincident rise in $bla_{OXA-48}$ in wastewater and broader ARG increases in
435 surface waters during a concurrent wet-weather period with confirmed CSOs. A broad
436 assessment of ARG concentrations in wastewater conducted over a limited timescale
437 found that variability in the wastewater resistome was driven by site-level heterogeneity,
438 potentially arising from differences in antimicrobial use between sewersheds.

439 **Viral pathogens**

440 The 2024 NFL Draft did not act as a superspreader event for respiratory pathogens.
441 Concentrations of SARS-CoV-2, IAV, IBV, and RSV remained steady or declined following
442 the event. No evidence of increased transmission was observed despite the substantial
443 increase in population in the monitored sewersheds and the mass gathering with increased
444 transmission risk. Multiple factors may have contributed to the observed lack of increased
445 transmission. The Draft was held outdoors and in large, well-ventilated buildings. This
446 would have helped to limit the potential for aerosol transmission despite the large
447 crowds[89]. Additionally, the Draft was held following the peak of the respiratory season in the
448 northern hemisphere. Immunity for the most relevant strains of respiratory virus was likely
449 high (acquired via infection or inoculation). The wastewater signal for most of the
450 monitored pathogens was already low, indicating that prevalence was already low,
451 reducing the probable number of infectious individuals attending Draft-related events. The
452 lack of immediate increase in signal over the Draft weekend may be related to the relatively
453 short duration of the Draft (~3 days) in comparison with viral incubation times (~5-6 days)[90].
454 The brevity of the mass gathering may not have allowed sufficient time for incubation or
455 widespread transmission. Our analysis also indicated that Draft related transmission was
456 low, with no significant increases in wastewater signal for any pathogens following the
457 event. These findings demonstrate that large numbers of individuals can congregate
458 without unreasonably increased risk of transmission if the gatherings occur outside of
459 respiratory seasons or proper precautions to mitigate spread are implemented. The
460 absence of a detectable signal does not imply complete absence of transmission; it does,
461 however, suggest that the mass gathering event did not lead to a widespread increase in
462 cases. Lack of extensive transmission is an important finding that can inform public health

463 decision-making and provide feedback on event timing and the types of transmission
464 mitigation strategies employed. Additionally, detection of transmission would be valuable
465 for informed rapid action, especially when clinical case reporting is not feasible or delayed.

466 **Event-associated increases in carbapenemase genes**

467 Unlike the monitored respiratory viruses, carbapenemase genes increased
468 measurably following the mass gathering, driven by a large increase in $bla_{OXA-48}$ signal. The
469 mass gathering event and influx of visitors were associated with a transient spike in the
470 concentration of a clinically important ARG in the wastewater system. A lack of increase in
471 any carbapenemase gene concentration at the spatially distinct control sites increases the
472 likelihood that Draft-related travel was responsible for the increase rather than seasonal
473 variability in ARG concentration. The increase in $bla_{OXA-48}$ observed in the present study may
474 be partially explained by Draft attendees arriving from regions where OXA-48-like
475 carbapenemases are more prevalent. These include parts of Europe, Africa, and the Middle
476 East[92]. International travel is an important driver of the dissemination of OXA-48-like
477 carbapenemases[93,94] and in non-endemic areas, infections are often imported, though this
478 modality may be changing[95]. Our results indicated that the increase in $bla_{OXA-48}$ was
479 transient with no evidence of a sustained increase. However, the large increase in $bla_{OXA-48}$
480 concentration was notable, especially given that the baseline ARG signal was highly
481 variable. This demonstrates that WES for ARGs may be sensitive to short term
482 perturbations and that mass gatherings may induce short term changes in load for select
483 ARGs. Wastewater flow was found to be a significant positive predictor of normalized ARG
484 concentration, potentially a result of surface inputs to the sewer system or the mobilization
485 of sewer biofilms[96,97].

486

487 **Stable resistome with site-level heterogeneity**

488 Multivariate analysis consistently indicated that the resistome structure in
489 wastewater was dominated by sampling site characteristics rather than changes
490 associated with the 2024 NFL Draft. This suggests that the influx of visitors during the 2024
491 NFL Draft did not significantly affect the resistome of the monitored sites in a way that was
492 detectable in this analysis. Likely, sewershed level drivers such as population
493 demographics, hospital effluent volumes, land use characteristics (i.e., amount of animal
494 agriculture), and antibiotic prescription rates played a key role in determining the
495 resistome. This was further supported by PCA loadings, which were dominated by common
496 markers of anthropogenic pollution, like *int1* and *sul1*[98,99]. These ARGs co-varied across
497 sites and sampling periods, indicating that the variation was driven by baseline pollution
498 levels. Most PC1 loadings had the same sign, supporting the notion of covariance of ARGs
499 being driven by variability in baseline pollution. ARG concentrations at the JEFF interceptor
500 (the sampling site most closely linked to Draft activities) were not influenced by the Draft.

501 Conclusions from this analysis must be interpreted with caution as group sizes were
502 uneven, sample sizes were small, and the study period was short. Combined, these limit
503 the statistical power of the current analyses to detect relatively small changes in ARG
504 concentration. Additionally, the OpenArray® has few targets compared to the diversity of
505 ARGs, limiting our ability to detect ARGs that may have been introduced by the Draft.
506 Incorporation of ultra deep metagenomic sequencing may allow for the detection of novel,
507 and low-abundance ARGs[100]. Longer-term data would help to confirm any Draft-associated
508 changes. The results of this study are not generalizable. Mass gathering events still have
509 the potential to contribute to ARG dissemination, especially if they are associated with
510 travel between jurisdictions with different antimicrobial prescribing practices.

511 **Environmental dissemination of ARGs**

512 Analyses revealed an increase in detection frequency and normalized concentration
513 for multiple ARGs in the Detroit River following the 2024 NFL Draft weekend. The Draft
514 event coincided with heavy precipitation, driving a CSO event. Detection probability

515 increased for clinically relevant ARGs including: *AAC(6')-Ib-cr, qnRS, tetA, mph(A),* and
516 $bla_{KPC}$. These ARGs are associated with a variety of antimicrobial agents, indicating broad,
517 rather than targeted increases in ARG detection following the Draft weekend. No gene ×
518 group interaction terms were significant in the GLMM, suggesting that the magnitude of the
519 increase was consistent between targets. The rise in crAssphage concentrations in the
520 post-Draft environmental samples and uniformity of detection probability increases across
521 gene targets indicate that sewage contamination from the CSO is a major cause of the
522 observed increase in ARG detections and abundance in the environmental samples. CSO
523 events in isolation have been found to increase environmental concentrations of
524 ARGs[101,102]. Mass gathering events can contribute to increased wastewater volumes and
525 ARG loads[103]. However, given that OpenArray® -based analysis of wastewater samples did
526 not detect a statistically significant increase in ARG concentrations attributable to the NFL
527 Draft, the observed increase in ARG in the environment was likely caused by the rainfall-
528 driven CSO events. The coincidence of the mass gathering event and the CSO may have
529 introduced ARGs to the environment, imported to the region by event attendees, thus
530 altering the watershed resistome. Such alterations have been observed in previous
531 studies[104].

532 Heterogeneity was observed among the sites of the sampling transect, with site-
533 specific responses to the CSO and mass gathering. Samples collected at the outlet of the
534 WEWTP exhibited evidence of saturated detection, accompanied by the highest
535 normalized ARG concentrations. These findings support that the WWTP outlet was a major
536 source of ARGs in the receiving waters with constitutively high ARG concentrations.
537 Inclusion of samples collected at the point source in data analysis obscured more subtle
538 changes in ARG concentrations at other sites. This observation indicates the importance of
539 site selection and highlights the complexity of interpretation for WES data in systems that
540 are influenced by persistent inputs. In these systems, measuring baseline contamination
541 levels is inherently challenging. Findings also indicated that the influence of the CSO was
542 not limited to the pollution source. Increased concentrations of ARGs were found at the
543 site upstream of the known WWTP outlet as well as the downstream sites. This observation

544 could be explained by environmental sewage contamination originating from CSO events
545 that occurred upstream within the Huron-Erie Corridor. Mass gatherings may increase the
546 consequences of rainfall events in combined sewer systems, leading to alterations in the
547 resistome of the receiving waters. Such alterations may have consequences for
548 downstream utilization of water resources[105].

549 Limitations of this analysis arise from the restricted temporal sampling and reliance
550 on RT-qPCR for ARG measurement. RT-qPCR cannot detect which pathogen is hosting an
551 ARG or if they are hosted on mobile genetic elements. Future work should incorporate
552 longer-term monitoring efforts, hydrological modelling for better source tracking and
553 should include metagenomic sequencing to help resolve ARG host identity.

554 **Comparison between OpenArray® and RT-qPCR**

555 Comparison of the OpenArray ®and RT-qPCR quantification of three
556 carbapenemase genes across two sample matrices ascertained the validity of the
557 OpenArray® platform for ARG surveillance. The OpenArray® can be used for ARG trend
558 assessment in concentrated wastewater matrices, but it is not directly quantitatively
559 interchangeable with RT-qPCR, due to lower sample volumes. Agreement between the two
560 methods was dependent on ARG abundance in the sample measured. Concordance
561 between methods was 100% in high-concentration wastewater samples but was poor for
562 environmental samples. Disagreement arose from non-detects by the OpenArray® rather
563 than quantitative disagreement between methods. This observation is consistent with the
564 approximately 600-fold smaller reaction volume (33nL vs 20μL) for the OpenArray®, which
565 lowers detection probability at low copy numbers. Thus, the OpenArray® has limited utility
566 for environmental monitoring without upstream concentration in the workflow[106–108].

567 Assessment of quantitative agreement between OpenArray® in high concentration
568 matrices also revealed significant discrepancies between methods. Passing-Bablok and
569 Demming regression both revealed systematic proportional and constant bias between
570 methods. Slopes greater than 1 and large negative intercepts are consistent with

underestimation of samples at low concentrations and progressive overestimation at higher concentrations (consistent with nanolitre scale inputs, but a more efficient assay).

Agreement between the OpenArray® and RT-qPCR platforms was target dependent with $bla_{KPC}$ showing the strongest quantitative agreement (CCC=0.94), indicating methodological interchangeability. However, for $bla_{NDM}$ and $bla_{OXA-48}$, overall agreement between methods was much lower (CCC=0.88 and CCC=0.75, respectively). For these targets, OpenArray® and RT-qPCR methods are not quantitatively interchangeable. However, strong correlations were found between OpenArray® data and RT-qPCR data for all tested targets (Table 7). These correlations support reliable trend tracking for OpenArray® and RT-qPCR despite differences in the absolute concentration measured. Tracking of trends over time is an important aspect of both wastewater-based surveillance and environmental monitoring, and despite the apparent quantitative issues with the OpenArray® platform, trend agreement is encouraging for the future development of the platform. The multitude of ARG targets to be monitored and high relative abundance in wastewater matrices make OpenArray® a promising platform for ARG monitoring in high concentration matrices with potential future applications for environmental monitoring with the implementation of pre-amplification and further methodological confirmations.

Low quantitative concordance between OpenArray® and RT-qPCR for $bla_{OXA-48}$ may help to explain why OpenArray® analysis failed to detect the spike in $bla_{OXA-48}$ that was detected via RT-qPCR. Optimization of multiplexed RT-qPCR allows for improved assay performance while cycling conditions for OpenArray® are set and uniform for all targets included on the chip. Additionally, OpenArray® analysis of the wastewater resistome relied on a limited number of samples while RT-qPCR benefited from a year-long survey of carbapenemase gene concentrations and a more sophisticated ITS modelling approach that attempted to account for baseline variability in carbapenemase concentrations.

## Conclusion

The main goals of this investigation were to determine whether WES is a viable tool for monitoring pathogen transmission dynamics associated with mass gathering events

599 and to determine if the 2024 NFL Draft led to increased pathogen transmission or ARG
600 dissemination. Findings provide support for the use of WES in this application, with results
601 of respiratory pathogen monitoring indicating no discernible increase in transmission
602 associated with the 2024 NFL Draft. WES to monitor trends in AMR is particularly promising
603 as it can capture a dimension of infectious diseases that are more difficult to track via
604 clinical surveillance methods. Additionally, environmental dissemination of ARGs is
605 impossible to track via clinical surveillance but can have implications for population
606 health. The ability of WES to detect transient resistome shifts makes the argument that it is
607 a valuable public health surveillance tool during mass gatherings. A recent study
608 investigated ARG load, diversity and dissemination in relation to mass gathering events[109].
609 Investigators found that the overall level of ARGs did not increase in relation to mass
610 gathering events. More importantly, they determined that mass gatherings could introduce
611 ARGs to local sewer systems that were previously absent. Findings of our investigation are
612 similar, albeit more methodologically limited, as we only measured select ARGs. Both our
613 investigation and the previous work found that ARG burden did not increase overall as a
614 result of the mass gathering but that the concentration of select genes might increase in a
615 transient manner and that the event itself may have led to the introduction of locally novel
616 ARGs. Notably, the wastewater signal observed in this study was not driven by a uniform
617 increase across all monitored targets. Instead, the response was selective, emphasizing
618 the importance of targeted surveillance strategies and careful interpretation of WES data in
619 event-based contexts. Dissemination of locally novel ARGs is concerning from a public
620 health perspective as it is likely to lead to increased numbers of antibiotic-resistant
621 infections or infections with novel resistance profiles. The combined evidence supports
622 WES as a reliable tool for validating the safety of mass gatherings regarding respiratory
623 spread while providing early insight into AMR dynamics and environmental dissemination
624 under infrastructure stress. Integrating WES with hydrologic context (rainfall, CSO
625 telemetry) can guide real-time operational responses (e.g., CSO management, advisories)
626 during future events.

627

**Acknowledgements**

Operators, Laboratory Team, and Managers of the following wastewater treatment facilities: Wastewater Resource Recovery Facility, Great Lakes Water Authority; Pollution Control, City of Windsor; Pollution Control Centre, Municipality of Leamington, Water Pollution Control Plants, City of Chatham and City of Thunder Bay. Funding in support of the Ontario Wastewater Surveillance Initiative was provided by the Ontario Ministry of Environment, Conservation, and Parks. Additional support was provided by the Public Health Agency of Canada's National Wastewater Surveillance Program (Contribution Agreement 2324-HQ-000197 to CGW, DDH, RS and RMM). The views expressed herein do not necessarily represent the views of the Public Health Agency of Canada.

**Citations**


1. Gonzalez, R. & Smith, J. Population-level health monitoring using wastewater surveillance. *Journal of Public Health Advances* **34**, 456–470 (2021).
2. Mao, K., Zhang, H. & Yang, Z. Wastewater-based epidemiology and community health: A review. *Environmental Research* **191**, 110351 (2020).
3. Sims, N. & Kasprzyk-Hordern, B. Future perspectives of wastewater-based epidemiology. *Environmental Health Journal* **50**, 123–135 (2020).
4. Hillary, L. S. *et al.* Monitoring SARS-CoV-2 in municipal wastewater to evaluate the success of lockdown measures for controlling COVID-19 in the UK. *Water Research* **200**, 117214 (2021).
5. Medema, G., Heijnen, L., Elsinga, G., Italiaander, R. & Brouwer, A. Presence of SARS-Coronavirus-2 RNA in Sewage and Correlation with Reported COVID-19 Prevalence in the Early Stage of the Epidemic in The Netherlands. *Environ. Sci. Technol. Lett.* **7**, 511–516 (2020).
6. Yanaç, K., Adegoke, A., Wang, L., Uyaguari, M. & Yuan, Q. Detection of SARS-CoV-2 RNA throughout wastewater treatment plants and a modeling approach to understand COVID-19 infection dynamics in Winnipeg, Canada. *Sci Total Environ* **825**, 153906 (2022).
7. Corchis-Scott, R. *et al.* Averting an Outbreak of SARS-CoV-2 in a University Residence Hall through Wastewater Surveillance. *Microbiol Spectr* **9**, e0079221 (2021).
8. Daughton, C. G. Wastewater surveillance: An emerging tool for epidemiology. *Environmental Science and Technology* **54**, 431–438 (2020).

9. Farkas, K., Hillary, L. S. & Malham, S. K. Wastewater surveillance as a tool for monitoring the SARS-CoV-2 pandemic. *Current Opinion in Environmental Science and Health* **17**, 14–20 (2020).
10. Tiwari, A. & Kumar, R. The renaissance of wastewater surveillance during the SARS-CoV-2 pandemic. *Epidemiological Reviews* **45**, 78–89 (2022).
11. Ahmed, W. *et al.* Occurrence of multiple respiratory viruses in wastewater in Queensland, Australia: Potential for community disease surveillance. *Sci Total Environ* **864**, 161023 (2023).
12. Corchis-Scott, R. *et al.* Wastewater Surveillance to Confirm Differences in Influenza A Infection between Michigan, USA, and Ontario, Canada, September 2022–March 2023 - Volume 30, Number 8—August 2024 - Emerging Infectious Diseases journal - CDC. *Emerging Infectious Diseases* **30**, (2024).
13. Galani, A. *et al.* SARS-CoV-2 wastewater surveillance data can predict hospitalizations and ICU admissions. *Science of The Total Environment* **804**, 150151 (2022).
14. Peccia, J. *et al.* Measurement of SARS-CoV-2 RNA in wastewater tracks community infection dynamics. *Nat Biotechnol* **38**, 1164–1167 (2020).
15. Hopkins, L. *et al.* Citywide wastewater SARS-CoV-2 levels strongly correlated with multiple disease surveillance indicators and outcomes over three COVID-19 waves. *Sci Total Environ* **855**, 158967 (2023).
16. Zhao, L. *et al.* Targeting a free viral fraction enhances the early alert potential of wastewater surveillance for SARS-CoV-2: a methods comparison spanning the transition between Delta and Omicron Variants in a large urban center. *fpubh* (2023).

17. Gerrity, D., Papp, K., Stoker, M., Sims, A. & Frehner, W. Early-pandemic wastewater surveillance of SARS-CoV-2 in Southern Nevada: Methodology, occurrence, and incidence/prevalence considerations. *Water Res X* **10**, 100086 (2020).
18. Yoo, B.-K., Iwamoto, R., Chung, U., Sasaki, T. & Kitajima, M. Economic Evaluation of Wastewater Surveillance Combined with Clinical COVID-19 Screening Tests, Japan. *Emerg Infect Dis* **29**, 1608–1617 (2023).
19. Wright, J., Driver, E. M., Bowes, D. A., Johnston, B. & Halden, R. U. Comparison of high-frequency in-pipe SARS-CoV-2 wastewater-based surveillance to concurrent COVID-19 random clinical testing on a public U.S. university campus. *Science of The Total Environment* **820**, 152877 (2022).
20. Safford, H. R., Shapiro, K. & Bischel, H. N. Wastewater analysis can be a powerful public health tool—if it's done sensibly. *Proceedings of the National Academy of Sciences* **119**, e2119600119 (2022).
21. Ngwira, L. G. *et al.* Cost of wastewater-based environmental surveillance for SARS-CoV-2: Evidence from pilot sites in Blantyre, Malawi and Kathmandu, Nepal. *PLOS Glob Public Health* **2**, e0001377 (2022).
22. National Academies of Sciences, E. *et al.* Wastewater Surveillance for COVID-19. in *Wastewater-based Disease Surveillance for Public Health Action* (National Academies Press (US), 2023).
23. Corchis-Scott, R. *et al.* Actionable wastewater surveillance: application to a university residence hall during the transition between Delta and Omicron resurgences of COVID-19. *Frontiers in Public Health* **11**, (2023).

24. Bivins, A. & Bibby, K. Wastewater Surveillance during Mass COVID-19 Vaccination on a College Campus. *Environ Sci Technol Lett* **8**, 792–798 (2021).
25. Mercier, E. *et al.* Municipal and neighbourhood level wastewater surveillance and subtyping of an influenza virus outbreak. *Sci Rep* **12**, 15777 (2022).
26. Zheng, X. *et al.* Wastewater Surveillance Provides Spatiotemporal SARS-CoV-2 Infection Dynamics. *Engineering* **40**, 70–77 (2024).
27. Jarvie, M. M., Nguyen, T. N. T., Southwell, B. & Wright, D. Leveraging wastewater surveillance to actively monitor Covid-19 community dynamics in rural areas with reduced reliance on clinical testing. *Applied Research* **3**, e202400012 (2024).
28. Memish, Z. A. *et al.* Mass gatherings medicine: public health issues arising from mass gathering religious and sporting events. *The Lancet* **393**, 2073–2084 (2019).
29. Suñer, C. *et al.* Association between two mass-gathering outdoor events and incidence of SARS-CoV-2 infections during the fifth wave of COVID-19 in north-east Spain: A population-based control-matched analysis. *Lancet Reg Health Eur* **15**, 100337 (2022).
30. Memish, Z. A. *et al.* Proactive surveillance for avian influenza H5N1 and other priority pathogens at mass gathering events. *The Lancet Public Health* **9**, e350–e352 (2024).
31. Verovšek, T., Krizman-Matasic, I., Heath, D. & Heath, E. Site- and event-specific wastewater-based epidemiology: Current status and future perspectives. *Trends in Environmental Analytical Chemistry* **28**, e00105 (2020).
32. Toro, L. *et al.* Pathogen prioritisation for wastewater surveillance ahead of the Paris 2024 Olympic and Paralympic Games, France. *Eurosurveillance* **29**, 2400231 (2024).

33. Saied, A. A. *et al*. Wastewater surveillance as an epidemiological tool at mass gathering events: A FIFA World Cup Qatar 2022 perspective and implication to other mass gathering events. *International Journal of Surgery* **109**, 574 (2023).

34. Kitajima, M., Murakami, M., Iwamoto, R., Katayama, H. & Imoto, S. COVID-19 wastewater surveillance implemented in the Tokyo 2020 Olympic and Paralympic Village. *Journal of Travel Medicine* **29**, taac004 (2022).

35. Nkambule, S., Street, R., Surujlal-Naicker, S., Johnson, R. & Mathee, A. Wastewater surveillance for SARS-CoV-2 during a mass sporting event in the City of Cape Town, Western Cape. *Front. Public Health* **12**, (2024).

36. El-Malah, S. S. *et al*. Leveraging wastewater surveillance for managing the spread of SARS-CoV-2 and concerned pathogens during FIFA World Cup Qatar 2022. *Heliyon* **10**, e30267 (2024).

37. Brighton, K., Fisch, S., Wu, H., Vigil, K. & Aw, T. G. Targeted community wastewater surveillance for SARS-CoV-2 and Mpox virus during a festival mass-gathering event. *Science of The Total Environment* **906**, 167443 (2024).

38. Sharma, A., Karande, M. & Zumla, A. Advancing sewage surveillance at mass gathering events for reducing transmission of antimicrobial resistant bacterial pathogens. *Travel Medicine and Infectious Disease* **54**, 102619 (2023).

39. Alexander, J., Hembach, N. & Schwartz, T. Evaluation of antibiotic resistance dissemination by wastewater treatment plant effluents with different catchment areas in Germany. *Sci Rep* **10**, 8952 (2020).

40. Karkman, A., Do, T. T., Walsh, F. & Virta, M. P. J. Antibiotic-Resistance Genes in Waste Water. *Trends Microbiol* **26**, 220–228 (2018).

41. Choi, P. M. *et al*. Wastewater-based epidemiology biomarkers: Past, present and future. *TrAC Trends in Analytical Chemistry* **105**, 453–469 (2018).

42. Keenum, I. *et al*. A framework for standardized qPCR-targets and protocols for quantifying antibiotic resistance in surface water, recycled water and wastewater. *Critical Reviews in Environmental Science and Technology* **52**, 4395–4419 (2022).

43. Hendriksen, R. S. *et al*. Global monitoring of antimicrobial resistance based on metagenomics analyses of urban sewage. *Nat Commun* **10**, 1124 (2019).

44. Harrop, E. *et al*. Spatiotemporal Variability in Wastewater-Derived Carbapenem-Resistance Genes from Diverse Municipal Sources in the Laurentian Great Lakes Catchment. Preprint at https://doi.org/10.21203/rs.3.rs-8206721/v1 (2026).

45. Lynggaard, C., Gogarten, J. F. & Jokelainen, P. Integrating environment into One Health approaches: Embracing the complexity. *One Health* **20**, 101021 (2025).

46. Greer, J. From Boardrooms to Block Parties: A Case Study on The Economic and Cultural Transformation of the NFL Draft. *Sport Economics Research* **2**, 29–44 (2025).

47. Williams, K. T. W. & Hall, J. C. The Impact of the 2024 NFL Draft on Hotel Demand. *JRAP* **55**, (2025).

48. Hutchinson, D. Here's how many people traveled at least 100 miles to attend NFL Draft in Detroit. *WDIV* (2024).

49. NCEI Past Weather Tool | Drought.gov. https://www.drought.gov/data-maps-tools/ncei-past-weather-tool.

50. CSO/SSO List - MiEnviro Portal. https://mienviro.michigan.gov/ncore/external/overflow/list.

51. Rosario, K., Symonds, E. M., Sinigalliano, C., Stewart, J. & Breitbart, M. Pepper Mild Mottle Virus as an Indicator of Fecal Pollution. *Appl Environ Microbiol* **75**, 7261–7267 (2009).

52. Maal-Bared, R. *et al.* Does normalization of SARS-CoV-2 concentrations by Pepper Mild Mottle Virus improve correlations and lead time between wastewater surveillance and clinical data in Alberta (Canada): comparing twelve SARS-CoV-2 normalization approaches. *Sci Total Environ* **856**, 158964 (2023).

53. Germovsek, E., Barker, C. I. & Sharland, M. What do I need to know about aminoglycoside antibiotics? *Arch Dis Child Educ Pract Ed* **102**, 89–93 (2017).

54. Krause, K. M., Serio, A. W., Kane, T. R. & Connolly, L. E. Aminoglycosides: An Overview. *Cold Spring Harb Perspect Med* **6**, a027029 (2016).

55. Holbrook, S. Y. L. & Garneau-Tsodikova, S. Evaluation of Aminoglycoside and Carbapenem Resistance in a Collection of Drug-Resistant Pseudomonas aeruginosa Clinical Isolates. *Microb Drug Resist* **24**, 1020–1030 (2018).

56. Zhao, S. *et al.* Epidemiology of and risk factors for mortality due to carbapenemase-producing organisms (CPO) in healthcare facilities. *J Hosp Infect* **110**, 184–193 (2021).

57. Bonomo, R. A. *et al.* Carbapenemase-Producing Organisms: A Global Scourge. *Clin Infect Dis* **66**, 1290–1297 (2018).

58. Carbapenemase Producing Enterobacteriaceae (CPE). *Public Health Ontario* http://www.publichealthontario.ca/en/Diseases-and-Conditions/Health-Care-Associated-Infections/CPE.

59. Shaikh, S., Fatima, J., Shakil, S., Rizvi, S. Mohd. D. & Kamal, M. A. Antibiotic resistance and extended spectrum beta-lactamases: Types, epidemiology and treatment. *Saudi J Biol Sci* **22**, 90–101 (2015).

60. Araten, A. H. *et al.* Cephalosporin resistance, tolerance, and approaches to improve their activities. *J Antibiot* **77**, 135–146 (2024).

61. Park, S. H. Third-generation cephalosporin resistance in gram-negative bacteria in the community: a growing public health concern. *Korean J Intern Med* **29**, 27–30 (2014).

62. Liguori, K. *et al.* Antimicrobial Resistance Monitoring of Water Environments: A Framework for Standardized Methods and Quality Control. *Environ Sci Technol* **56**, 9149–9160 (2022).

63. 2021 AWaRe classification. https://www.who.int/publications-detail-redirect/2021-aware-classification.

64. Hooper, D. C. & Jacoby, G. A. Mechanisms of drug resistance: quinolone resistance. *Ann N Y Acad Sci* **1354**, 12–31 (2015).

65. Camins, B. C. *et al.* The clinical impact of fluoroquinolone resistance in patients with E coli bacteremia. *J Hosp Med* **6**, 344–349 (2011).

66. Salah, F. D. *et al.* Distribution of quinolone resistance gene (qnr) in ESBL-producing Escherichia coli and Klebsiella spp. in Lomé, Togo. *Antimicrobial Resistance & Infection Control* **8**, 104 (2019).

67. Peirano, G. & Pitout, J. D. D. Fluoroquinolone-Resistant Escherichia coli Sequence Type 131 Isolates Causing Bloodstream Infections in a Canadian Region with a Centralized Laboratory System: Rapid Emergence of the H30-Rx Sublineage. *Antimicrobial Agents and Chemotherapy* **58**, 2699–2703 (2014).
68. Yang, P. *et al.* Association between the rate of fluoroquinolones-resistant gram-negative bacteria and antibiotic consumption from China based on 145 tertiary hospitals data in 2014. *BMC Infectious Diseases* **20**, 269 (2020).
69. Kibwana, U. O. *et al.* Fluoroquinolone resistance among fecal extended spectrum βeta lactamases positive Enterobacterales isolates from children in Dar es Salaam, Tanzania. *BMC Infectious Diseases* **23**, 135 (2023).
70. Selim, S. Mechanisms of gram-positive vancomycin resistance (Review). *Biomed Rep* **16**, 7 (2022).
71. Patel, S., Preuss, C. V. & Bernice, F. Vancomycin. in *StatPearls* (StatPearls Publishing, Treasure Island (FL), 2024).
72. Mühlberg, E. *et al.* Renaissance of vancomycin: approaches for breaking antibiotic resistance in multidrug-resistant bacteria. *Can. J. Microbiol.* **66**, 11–16 (2020).
73. Patel, P. H. & Hashmi, M. F. Macrolides. in *StatPearls* (StatPearls Publishing, Treasure Island (FL), 2024).
74. Bengtsson-Palme, J. *et al.* Industrial wastewater treatment plant enriches antibiotic resistance genes and alters the structure of microbial communities. *Water Research* **162**, 437–445 (2019).

75. Wang, H. *et al.* Characterization of resistance genes and plasmids from sick children caused by Salmonella enterica resistance to azithromycin in Shenzhen, China. *Front. Cell. Infect. Microbiol.* **13**, (2023).

76. Schwartz, K. L. *et al.* Regional variability in outpatient antibiotic use in Ontario, Canada: a retrospective cross-sectional study. *CMAJ Open* **6**, E445–E452 (2018).

77. Siddiqui, A. H. & Koirala, J. Methicillin-Resistant Staphylococcus aureus. in *StatPearls* (StatPearls Publishing, Treasure Island (FL), 2024).

78. Snitser, O. *et al.* Ubiquitous selection for mecA in community-associated MRSA across diverse chemical environments. *Nat Commun* **11**, 6038 (2020).

79. Tyson, G. H., Li, C., Hsu, C.-H., Bodeis-Jones, S. & McDermott, P. F. Diverse Fluoroquinolone Resistance Plasmids From Retail Meat E. coli in the United States. *Front. Microbiol.* **10**, (2019).

80. Ovung, A. & Bhattacharyya, J. Sulfonamide drugs: structure, antibacterial property, toxicity, and biophysical interactions. *Biophys Rev* **13**, 259–272 (2021).

81. Vester, B. The *cfr* and cfr-like multiple resistance genes. *Research in Microbiology* **169**, 61–66 (2018).

82. Mirnezami, M., Ranjbar, R., Niakan, M. & Ahmadi, M. H. Frequency of Antimicrobial Resistance and Class 1 and 2 Integrons in Escherichia Coli Strains Isolated from Urinary Tract Infections. *Iran J Pharm Res* **19**, 282–287 (2020).

83. Racewicz, P. *et al.* Prevalence and characterisation of antimicrobial resistance genes and class 1 and 2 integrons in multiresistant Escherichia coli isolated from poultry production. *Sci Rep* **12**, 6062 (2022).

84. Stachler, E. *et al.* Quantitative CrAssphage PCR Assays for Human Fecal Pollution Measurement. *Environ. Sci. Technol.* **51**, 9146–9154 (2017).

85. Langeveld, J. *et al.* Normalisation of SARS-CoV-2 concentrations in wastewater: The use of flow, electrical conductivity and crAssphage. *Sci Total Environ* **865**, 161196 (2023).

86. R Core Team. *R: A Language and Environment for Statistical Computing*. (R Foundation for Statistical Computing, Vienna, Austria, 2025).

87. Wickham, H. *et al.* Welcome to the tidyverse. *Journal of Open Source Software* **4**, 1686 (2019).

88. McBride, G. & others. A proposal for strength-of-agreement criteria for Lin's concordance correlation coefficient. *NIWA client report: HAM2005-062* **45**, 307–310 (2005).

89. Bulfone, T. C. *et al.* Outdoor Activities Associated with Lower Odds of SARS-CoV-2 Acquisition: A Case–Control Study. *Int J Environ Res Public Health* **19**, 6126 (2022).

90. Lessler, J. *et al.* Incubation periods of acute respiratory viral infections: a systematic review. *The Lancet Infectious Diseases* **9**, 291–300 (2009).

91. Alandijany, T. A. Respiratory viral infections during Hajj seasons. *Journal of Infection and Public Health* **17**, 42–48 (2024).

92. Boyd, S. E., Holmes, A., Peck, R., Livermore, D. M. & Hope, W. OXA-48-Like β-Lactamases: Global Epidemiology, Treatment Options, and Development Pipeline. *Antimicrobial Agents and Chemotherapy* **66**, e00216-22 (2022).

93. Kajova, M., Khawaja, T., Kainulainen, K. & Kantele, A. Travel-associated carbapenemase-producing Enterobacterales: Epidemiology and risk factors in a Finnish cohort. *Travel Medicine and Infectious Disease* **68**, 102926 (2025).

94. Pitout, J. D. D., Peirano, G., Kock, M. M., Strydom, K.-A. & Matsumura, Y. The Global Ascendency of OXA-48-Type Carbapenemases. *Clin Microbiol Rev* **33**, e00102-19 (2019).

95. Peirano, G. & Pitout, J. D. D. Rapidly spreading Enterobacterales with OXA-48-like carbapenemases. *Journal of Clinical Microbiology* **63**, e01515-24 (2025).

96. Auguet, O. *et al.* Sewers as potential reservoirs of antibiotic resistance. *Science of The Total Environment* **605–606**, 1047–1054 (2017).

97. Nahum, Y., Muhvich, J., Morones-Ramirez, J. R., Casillas-Vega, N. G. & Zaman, M. H. Biofilms as potential reservoirs of antimicrobial resistance in vulnerable settings. *Front Public Health* **13**, 1568463 (2025).

98. Haenelt, S. *et al.* The fate of sulfonamide resistance genes and anthropogenic pollution marker intI1 after discharge of wastewater into a pristine river stream. *Front Microbiol* **14**, 1058350 (2023).

99. Gillings, M. R. *et al.* Using the class 1 integron-integrase gene as a proxy for anthropogenic pollution. *ISME J* **9**, 1269–1279 (2015).

100. Rushford, C. *et al.* Untargeted longitudinal ultra deep metagenomic sequencing of wastewater provides a comprehensive readout of expected and unexpected viral pathogens. 2025.10.27.25338874 Preprint at https://doi.org/10.1101/2025.10.27.25338874 (2025).

896 101. Kaeseberg, T. *et al.* Hot spots of antibiotic tolerant and resistant bacterial
897 subpopulations in natural freshwater biofilm communities due to inevitable urban
898 drainage system overflows. *Environmental Pollution* **242**, 164–170 (2018).
899 102. Morina, J. C. & Franklin, R. B. Drivers of Antibiotic Resistance Gene Abundance in an
900 Urban River. *Antibiotics (Basel)* **12**, 1270 (2023).
901 103. Pao, L. T., Tashani, M., King, C., Rashid, H. & Khatami, A. Antimicrobial Resistance
902 Associated with Mass Gatherings: A Systematic Review. *Trop Med Infect Dis* **10**, 2
903 (2024).
904 104. Wang, C., Myshkevych, Y., Wang, T., Monjed, M. K. & Hong, P.-Y. Wastewater
905 surveillance unveils the impact of mass gatherings on antimicrobial resistance after the
906 COVID-19 pandemic in Saudi Arabia. *Nat Water* **3**, 693–703 (2025).
907 105. Li, Z. *et al.* The Environmental Lifecycle of Antibiotics and Resistance Genes:
908 Transmission Mechanisms, Challenges, and Control Strategies. *Microorganisms* **13**,
909 2113 (2025).
910 106. Ishii, S. *et al.* Microfluidic Quantitative PCR for Simultaneous Quantification of
911 Multiple Viruses in Environmental Water Samples. *Applied and Environmental*
912 *Microbiology* **80**, 7505–7511 (2014).
913 107. Ishii, S., Segawa, T. & Okabe, S. Simultaneous Quantification of Multiple Food- and
914 Waterborne Pathogens by Use of Microfluidic Quantitative PCR. *Appl Environ Microbiol*
915 **79**, 2891–2898 (2013).
916 108. Sekovanić, A. *et al.* Pre-amplification as a method for improvement of quantitative
917 RT-PCR analysis of circulating miRNAs. *Biochem Med (Zagreb)* **31**, 010901 (2021).

109. Wang, C., Myshkevych, Y., Wang, T., Monjed, M. K. & Hong, P.-Y. Wastewater surveillance unveils the impact of mass gatherings on antimicrobial resistance after the COVID-19 pandemic in Saudi Arabia. *Nat Water* **3**, 693–703 (2025).